

Disulfide bond based cascade reduction-responsive Pt(IV) nanoassemblies for improved anti-tumor efficiency and biosafety

Xiao Kuang, Dongxu Chi, Jinbo Li, Chunlin Guo, Yinxian Yang, Shuang Zhou, Cong Luo, Hongzhuo Liu, Zhonggui He, Yongjun Wang*

Department of Pharmaceutics, Wuya College of Innovation, Shenyang Pharmaceutical University, Shenyang, 110016, China

ARTICLE INFO

Keywords:

Disulfide bond
Oxaliplatin
Prodrug
Nanoassemblies
Biosafety

ABSTRACT

The platinum-based drugs prevail in the therapy of malignant tumors treatment. However, their clinical outcomes have been heavily restricted by severe systemic toxicities. To ensure biosafety and efficiency, herein, we constructed a disulfide bond inserted Pt(IV) self-assembled nanoplatform that is selectively activated by rich glutathione (GSH) in tumor site. Disulfide bond was introduced into the conjugates of oxaliplatin (IV) and oleic acid (OA) which conferred cascade reduction-responsiveness to nanoassemblies. Disulfide bond cleavage and reduction of Pt(IV) center occur sequentially as a cascade process. In comparison to oxaliplatin solution, Pt(IV) nanoparticles (NPs) achieved prolonged blood circulation and higher maximum tolerated doses. Furthermore, Oxa(IV)-SS-OA prodrug NPs exhibited potent anti-tumor efficiency against 4T1 cells and low toxicities in other normal tissues, which offers a promising nano-platform for potential clinical application.

1. Introduction

It has been more than four decades since the first prototype of platinum drug, cisplatin, was approved by the FDA. Today platinum-associated cancer therapies occupy an essential and irreplaceable proportion in clinic [1]. The activity of platinum compounds arises from the formation of cross-links *via* coordination with purine bases of DNA, which inhibit the biofunction of DNA and RNA polymerases and subsequently initiate a series of reactions that lead to cell apoptosis. Reactions with off-target Pt(II) species in normal tissues result in severe toxicities including nephrotoxicity, myelosuppression, peripheral neuropathy and ototoxicity [2], which provide an impetus to discover safer candidates or combined therapeutics [3]. Oxaliplatin, as the only third-generation platinum drug approved in clinic so far for treatment of advanced colorectal cancer with leucovorin and fluorouracil (FOLFOX), is characterized with the least nephrotoxic and much less other toxicities than cisplatin and carboplatin [4]. Nonetheless, high rate of peripheral neuropathy [5,6] occurred in patients after oxaliplatin administration, which is often responsible for limited tolerated dose and unfavorable therapy interruption [7]. Though preventive tactics, such as Ca/Mg infusions, were recommended to be a typical effective method to alleviate oxaliplatin-induced neurotoxicity, clinical studies demonstrated that

acute neurotoxicity of oxaliplatin could not be precluded by Ca/Mg infusions [8]. Adverse reactions of oxaliplatin have still hindered its clinical application.

In order to alleviate the clinical side effects and improve the therapeutic index, hundreds of chemical entities and platinum-based drug delivery strategies have been explored for potential application. Over the past few decades, a surge of Pt(IV) complexes have emerged in various fields. With kinetically more inert biochemical property as compared to Pt(II) compound, Pt(IV) prodrug become less reactive towards endogenous molecules, which consequently improved stability in blood circulation [9,10] and thus minimizing undesired toxicity of chemotherapy [2,11]. Reduction from Pt(IV) to active Pt(II) complexes were activated by reductants like ascorbate, glutathione and metallothionein that are overexpressed in almost all types of tumor cells. In addition, both axial orientations of Pt(IV) can be modified with a variety of functional ligands to give versatile delivery vehicle. Desired and tunable physicochemical properties such as lipophilicity, molecule weight and spatial microstructure are available in Pt(IV) platform to achieve high uptake or accumulation in tumor site [12]. Furthermore, different ligand types and multifunction of axial molecules endow Pt(IV) prodrug with targeting ability [13–15] or convenience of combined chemotherapy [16]. However, poor tumor selectivity and insufficient

* Corresponding author at: Department of Pharmaceutics, Wuya College of Innovation, Shenyang Pharmaceutical University, No. 103 Wenhua Road, Shenyang, 110016, China.

E-mail address: wangyongjun@syphu.edu.cn (Y. Wang).

<https://doi.org/10.1016/j.colsurfb.2021.111766>

Received 3 February 2021; Received in revised form 18 March 2021; Accepted 10 April 2021

Available online 15 April 2021

0927-7765/© 2021 Elsevier B.V. All rights reserved.

activity preclude Pt(IV) prodrug from exerting maximized efficiency in cancer treatment.

Compared to normal cells, glutathione (GSH) is overexpressed in almost all cancer cell lines [17], which is 1000-fold higher in tumor than that in the blood circulation and at least 4-fold higher than normal tissues [18]. Based on this, reduction-sensitive drug delivery systems (DDS) has been actively investigated. Among them, disulfide bond is increasingly acting as responsive linkers of DDS and proved to be cleaved and reduced into the hydrophilic thiol by GSH [19]. The reduction procedure promoted by elevated GSH level is much easier to proceed in tumor cells, facilitating the release of active pharmaceutical ingredient. In contrast, delayed drug release confirmed by lower GSH level in normal cells give rise to differential cytotoxicity and tumor selectivity. We have developed several DDS characterized by enhanced antitumor efficiency and alleviated systemic toxicity in the past few years [20–24]. It has been demonstrated that disulfide bond make DDS a more powerful tool to achieve accelerated drug release and enhanced tumor selectivity.

Unsaturated fatty acids (UFAs) are essential component of human body and play an important role in physiological functions such as regulation of membrane fluidity, reducing blood viscosity and brain nutrition to enhance memory [25]. In addition, tumor cells incline to ingest much more unsaturated fatty acids than normal cells due to unlimited proliferation. Therefore, with innate "nutritional targeting" effect and good biocompatibility, UFAs have been extensively used for the rational design of unsaturated fatty acids based drug delivery strategies in cancer therapy to improve prodrug properties and drug delivery efficiency [26].

Herein, we proposed a cascade reduction-sensitive Pt(IV) prodrug where disulfide bond was introduced into conjugate of oxaliplatin and oleic acid which is denoted as Oxa-SS-OA (Fig. 1). Disulfide bond guided Pt(IV) prodrug is capable of self-assembling into stable nanoparticles in water. After internalized into tumor cells, Oxa-SS-OA NPs can be activated selectively by GSH and release oxaliplatin in tumor cells. In response to reductive stimuli in 4T1 cells, Pt(IV) species are released from nanoassemblies after cleavage of disulfide bond. Then Oxa(IV) converted to active oxaliplatin by similar GSH-consuming procedure, which features a cascade reduction process mediated by GSH. It is noteworthy that Pt(IV) prodrug NPs exhibited higher maximum tolerated dose and prolonged blood circulation. Especially, Oxa-SS-OA NPs showed better antitumor efficiency than ester bond-based prodrug and free oxaliplatin. With impressive tumor selective activation and enabled biosafety, disulfide bond guided Pt(IV) nanoassemblies provide a

powerful delivery tool for platinum drugs.

2. Materials and methods

2.1. Materials

Oxaliplatin, oleic acid and dithiodiglycolic acid were obtained from Aladdin (Shanghai, China). H_2O_2 , acetic anhydride (Ac_2O) and ethylene glycol were purchased from Aladdin (Shanghai, China). 4-dimethylaminopyridine (DMAP), 1-hydroxybenzotriazole (HOBT) and 1-Ethyl-3-(3-dimethylaminopropyl)-carbodiimide hydrochloride (EDCI) were obtained from Chemlin Pharm Co. Ltd. (Nanjing, China). DSPE-PEG₂₀₀₀ were obtained from AVT (Shanghai) Pharmaceutical Co., Ltd. Coumarin-6 (C-6), glutathione (GSH), BCA protein assay kit and GSH and GSSG assay kit were procured from Solarbio Science & Technology co., Ltd (Beijing, China).

2.2. Synthesis of Pt(IV) prodrugs

The original reduction-responsive oxaliplatin-oleic acid conjugate Oxa-SS-OA was synthesized by tethering OA to oxaliplatin by disulfide bond. And non-sensitive Pt(IV) prodrug Oxa-OA conjugating via ester bond was directly synthesized by coupling OA to the axial hydroxyl of oxaliplatin. The reduction-responsive and non-responsive Pt(IV) nanoparticles were synthesized following our previously reported method [22,27]. All reactions were kept under nitrogen and against light. Chemical structures of all compounds were confirmed by MS and 1H NMR.

Specifically, oxaliplatin (0.5 mmol) was dissolved in 10 mL H_2O under 50 °C, followed by addition of 1 mL 30 % H_2O_2 and stirring for 3 h. The reaction solution was put under 4 °C overnight for recrystallization, the precipitation was collected and washed with ice-cold ethanol and diethyl ether sequentially. And the product was dried to give a white powder of Oxa(IV)-2OH (yield: 64.3 %).

Then oleic acid (OA, 0.6 mmol) and EDCI (1 mmol) were dissolved in DMF with stirring for 30 min under ice bath to activate $-COOH$ of OA. Oxa(IV)-2OH (0.5 mmol) dispersed in 20 mL DMF, followed by addition of activated OA and DMAP (0.2 mmol). The total solution was kept stirring for 12 h at 30 °C. The resulting solution was filtered, evaporated to 2 mL, and washed with acetone and diethyl ether. The precipitate was collected, washed with diethyl ether, and dried under vacuum to obtain Oxa(IV)-OA (yield: 53.6 %).

Oxa(IV)-SS-OA was prepared as following steps: OA (5 mmol,

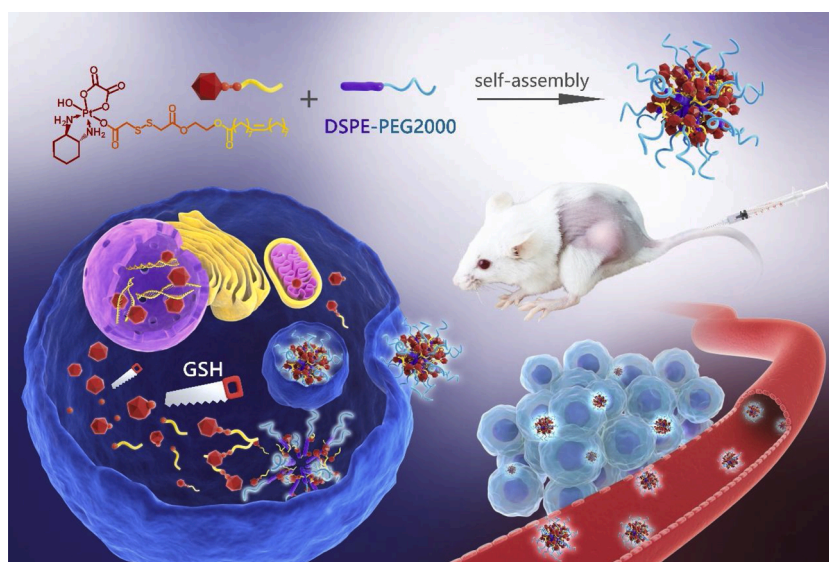


Fig. 1. Schematic representation. Disulfide-bond bridged Oxa-SS-OA prodrug nanoassemblies for cancer therapy.

dissolved in 2 mL methylbenzene) and p-toluenesulfonic acid (0.5 mmol, dissolved in 15 mL ethylene glycol) were added in one three-necked flask under agitation at 110 °C for 2 h. The product oleic acid 2-hydroxyethyl ester was purified by silica gel column chromatography (ethyl acetate: hexane = 1:32). 2,2'-thiobisacetic acid anhydride was obtained by the dehydration of dithiodiglycolic acid in acetic anhydride. EDCI-activated Oleic acid 2-hydroxyethyl ester (0.6 mmol), 2,2'-thiobisacetic acid anhydride (1 mmol) and DMAP (0.2 mmol) were dissolved in dichloromethane with stirring at 25 °C for 12 h. Then preparative liquid chromatography was applied to purify product OA-SS-COOH. 0.6 mmol EDCI-activated OA-SS-COOH was dissolved in DMF with addition of 0.5 mmol Oxa(IV)-2OH and 0.2 mmol DMAP. The final reaction was stirred overnight. The resulting solution was filtered, evaporated to 2 mL, and added to 50 mL diethyl ether. The precipitate was collected, washed with acetone and diethyl ether three times, and dried under vacuum to yield Oxa-SS-OA (yield: 47.3 %).

2.3. Preparation and characterization of Pt(IV) self-assembled nanoparticles

A facile nano-precipitation method was introduced to prepare self-assembled Pt(IV) nanoparticles. Briefly, 4 mg of Pt(IV) prodrug Oxa-OA or Oxa-SS-OA were dissolved in 0.2 mL ethanol solution containing 0.7 mg DSPE-PEG₂₀₀₀ to give a final polymer mass ratio of 15 %. Then the mixed liquor was pipetted dropwise into 2 mL water with agitation of 600 rpm to gain nanoparticles Oxa-OA NPs or Oxa-SS-OA NPs. Then all NPs were evaporated under vacuum at 30 °C to remove ethanol remaining. Non-PEGylated Oxa-OA and Oxa-SS-OA NPs were also prepared with the same method except that DSPE-PEG₂₀₀₀ was not added. Coumarin-6-labeled Pt(IV) prodrug nanoparticles were also prepared by transferring the solution of prodrugs, Coumarin-6 and DSPE-PEG₂₀₀₀ in ethanol to deionized water dropwise. The NPs characterization including particle size, PDI and zeta potential were confirmed and NPs morphology was observed by transmission electron microscope (TEM). And inductively coupled plasma mass spectrometry (ICP-MS) was applied for evaluating drug loading capacity of Pt(IV) NPs. Pre-processing methods of sample preparation before measurement by ICP-MS were provided from Sci-Tech innovation Co. Ltd (Qingdao, China).

2.4. Colloidal stability

To gain insight on the colloidal stability of the Pt(IV) NPs, nano-formulation was diluted 20 fold in PBS 7.4 containing 10 % FBS. The suspensions were incubated at 37 °C with gentle shaking. At prescriptive 0, 2, 4, 6, 8, 12 h intervals, the particle size was measured by Zetasizer (n = 3). Meanwhile, 1 mL of nano-formulation was also added to 20 mL 5% glucose and RPMI 1640 medium under room temperature which were measured by Zetasizer (n = 3) within 7 days.

2.5. In vitro drug release

The release of platinum from NPs was investigated under shaking (100 rpm) at 37 °C in different media, 10 mM PBS 7.4 containing 10 mM GSH. Typically, 1 mL of Oxa-OA NPs or Oxa-SS-OA NPs dispersions (2 mg/mL) in dialysis bag (MWCO 1000 D) was immersed in 20 mL of release media. The release profiles were measured at different time intervals: 1, 2, 4, 8, 12, and 24 h. At desired time points, 1 mL sample was analyzed and replaced with the equal fresh media. Platinum content was determined by ICP-MS.

2.6. Cell culture

L-02, RM-1 and 4T1 cells were originally purchased from Cell Resource Center, Shanghai Institutes for Biological Sciences, Chinese Academy of Sciences. L-02, RM-1 and 4T1 cells were cultured in routine

medium consisted of RPMI 1640, 10 % FBS, penicillin (30 mg/mL) and streptomycin (100 µg/mL). All cells were maintained in a humidified atmosphere of 5% CO₂ at 37 °C. Cells in culture medium were monitored by using an Eclipse Ti-U inverted microscope (Nikon Corp., Tokyo, Japan).

2.7. Cytotoxicity assay

L-02, RM-1 and 4T1 cells, after cultivation in 96-well plates at a density of 3×10^3 cells/well for 12 h, were treated with a series of dilution of free oxaliplatin, Pt(IV) solution and Pt(IV) NPs at various concentrations. After 24, 48 and 72 h incubation, 20 µL MTT (0.5 %) was added and incubated for 4 h. Then 200 µL DMSO was added to dissolve the formazan after medium abandoned. The absorbance was measured at 570 nm using a microplate reader.

2.8. Cell uptake and intracellular drug accumulation

Cells were seeded in 12-well plates with a density of 1×10^5 cells/well for 24 h. The medium was replaced with fresh medium containing free C-6, C-6-labeled Oxa-OA NPs and Oxa-SS-OA NPs with equivalent C-6 concentration of 250 ng mL⁻¹ for 0.5 or 4 h at 37 °C. And the cells without any treatment were utilized as control. After that, the fluorescence value of was analyzed by fluorescence activated cell sorting (FACS) analysis (Becton Dickinson, Germany). Meanwhile, 4T1 cells were cultured on 14-mm cover glasses and incubated with the same three formulations for 0.5 or 4 h respectively. Cells were fixed with 4% paraformaldehyde for 10 min and then labeled with Hoechst 33,342 for 10 min. Finally, the cells were observed by confocal laser scanning microscopy (CLSM, Nikon, Japan). And Pt content in 4T1 cells treated by oxaliplatin solution, Oxa-OA NPs and Oxa-SS-OA NPs was also detected by ICP-MS and cell quantitation was confirmed by BCA protein assay kit (Solarbio Co. Ltd.).

2.9. Determination of GSH and GSSG content inside cells

L-02, RM-1 and 4T1 cells were seeded in 12-well plates at 24 h, 10 µM Pt concentration of various formulations were transferred to each well for 12 h and then cells were divided into two groups after digestion. One was subjected to BCA protein content assay and the other for GSH and GSSG content assay by GSH and GSSG assay kits (Solarbio Co. Ltd.).

2.10. Determination of nucleus DNA-Pt adduct

4T1 cells were incubated with 6-well plates, cultured for 24 h, and then 10 µM Pt equivalence of different drugs (oxaliplatin, Oxa-OA NPs and Oxa-SS-OA NPs) were added incubated for another 12 h. The medium was removed and cells was gathered by centrifugation. Nucleus DNA was extracted with mammalian genomic DNA extraction kit (NEST Biotechnology) and digested with 1 mL of concentrated nitric acid at 80 °C overnight. Then the Pt concentration was determined by ICP-MS.

2.11. Animals

All of the animals were obtained from the Laboratory Animal Center of Shenyang Pharmaceutical University (Shenyang, Liaoning, China). All of the animal experiments were conducted according to the Guidelines for the Care and Use of Laboratory Animals approved by the Institutional Animal Ethical Care Committee (IAEC) of Shenyang Pharmaceutical University.

2.12. In vivo pharmacokinetics

Male Sprague-Dawley rats (200–250 g) were used to evaluate the pharmacokinetic profiles of Pt(IV) prodrug nanoassemblies. Prior to the experiments, the rats were fasted for 12 h with free access to water. The

animals were intravenously administered oxaliplatin solution, Oxa-OA NPs and Oxa-SS-OA at 3 mg Pt/kg ($n = 5$). At predetermined time points (15 min, 1, 4, 8, 12 h), blood samples were collected and extracted to obtain the plasma. Nitric acid (HNO_3 , 65 %, supra pure) was added into the plasma and allowed them to digest overnight. Then the samples were heated to remove HNO_3 . Then Pt concentration was measured with ICP-MS.

2.13. *In vivo* biodistribution

The *in vivo* distribution behaviors of Pt(IV) NPs into tumor and other organs were assessed in 4T1 tumor-bearing Balb/c mice (female, $n = 3$). Mice with subcutaneous tumors of approximately 400 mm³ were subjected to tail vein injection of oxaliplatin solution, Oxa-OA NPs and Oxa-SS-OA at 6 mg Pt/kg. At 4 and 12 h after dosing, mice were sacrificed followed by the organs (heart, liver, spleen, lung and kidney) and tumors immediately harvested. Then organs and tumors were washed in the saline, weighted and sheared by a tissue homogenizer. Pt concentration in tissues and tumors were analyzed by ICP-MS.

2.14. *In vivo* antitumor efficacy and systematic toxicity investigation

Maximum tolerated dose (MTD) was determined before antitumor efficacy investigation was conducted. Briefly, a series of doses of different formulations were i.v. injected into female Balb/c mice ($n = 3$ each group) every other day. Total four injections were carried out on the premise of no systemic toxicity observed. Body weights of mice were monitored and the maximal dosage administrated by mice group was determined as MTD if there were no more than 15 % weight loss of every mouse. Then 4T1 cells with a density of 5×10^6 cells per 100 μL were injected subcutaneously on female Balb/c mice. When tumor volume reached approximately 150 mm³, 4T1 tumor-bearing Balb/c mice were randomly divided into 4 groups ($n = 6$) and intravenously injected with 5% glucose solution as control group, oxaliplatin solution, Oxa-OA NPs and Oxa-SS-OA NPs at 6 mg Pt/kg. The i.v. administration schedule included total 4 times injection at 6-day intervals and the first injection was designated as day 0. Tumor volume and body weight was measured every other day. After tumor monitoring, all mice (6 mg Pt/kg) were euthanized and their blood samples were collected for hepatorenal function test (ALT, AST, BUN and CREA), tissues (heart, liver, spleen, lung, and kidney) separated for H&E staining. Tumors were harvested and weighed after euthanasia.

2.15. Behavioral assessment of mechanical hypersensitivity

The behavior investigation was conducted to evaluate oxaliplatin-induced peripheral neuropathy in SD rats subject to administration of oxaliplatin solution, Oxa-OA NPs and Oxa-SS-OA NPs. An *in vivo* model for oxaliplatin-induced peripheral neurotoxicity (increased sensitivity to mechanical force) was used [28] and neurotoxicity that developed after days following serial intravenous (i.v.) injections of oxaliplatin solution were recorded.

Sensitivity baseline of normal rats to mechanical stimuli was established by measuring 3 times before administration. Rats were randomly assigned to 4 treatment groups (5% glucose, oxaliplatin solution, Oxa-OA NPs and Oxa-SS-OA NPs, $n = 10$). Repeated dosing of 5% glucose and different formulations at the same dose of 2 mg Pt/kg (twice a week for a total of 4 i.v. injections) was launched to induce neuropathy. Sensitivity thresholds of each animal measurement was performed before drug administration.

Specifically, rats were placed in individual transparent boxes and get accustomed for 30 min. Mechanical paw withdrawal threshold (PWT) of hindpaw in response to the vertical force of von Frey filaments was recorded. A series of calibrated von Frey filaments (eleven levels ranging from 0.6–60 g, U.S. North Coast NC12775–99) were applied perpendicularly to the plantar surface of the hindpaw with a force to bend the

filaments for 10 s until paw withdraw as a response. In presence of a response, the filament of the next lower force was applied. And in the absence of a response, the filament of the next greater force was applied. To avoid injury during tests, the cutoff strength of the von Frey filament was 60 g. Each trial was repeated 3 times at approximately 2-min intervals. The mean value was used as the force produced a withdrawal response and recorded. And the body weights of all groups were also recorded every week.

2.16. Statistical analysis

All quantitative data are expressed as the mean \pm SD. Statistical analysis was performed with Student's *t*-test and one-way ANOVA. (* $p < 0.05$, ** $p < 0.01$, *** $p < 0.001$).

3. Results and discussion

3.1. Synthesis of Pt(IV) prodrugs

Unsaturated fatty acids based drug delivery strategies, characterized by favorable biocompatibility and native tumor-targeting effect, have been prevalently applied for the rational design of prodrug chemotherapy [26,29]. Several prodrugs have already successfully had access to clinical trials [26].

In this research, a GSH-responsive oxaliplatin prodrug monomer, Oxa-SS-OA, was synthesized by introducing a GSH-cleavable disulfide functional moiety to covalently bond oleic acid and oxaliplatin. Synthesis routes of Pt(IV) prodrug and chemical structures confirmed by MS and ¹H NMR were shown in Fig. 2A and Figure S1 and S2.

3.2. Preparation and characterization of Pt(IV) self-assembled nanoparticles

Both synthesized Oxa-OA and Oxa-SS-OA are able to self-assemble into NPs in aqueous solution *via* nanoprecipitation. In contrast, free oxaliplatin disperse in water uniformly suggesting the essential part of oleic acid moiety in the nanoparticle-forming process. The size distribution and morphology of nanoassemblies were characterized by TEM and DLS in Fig. 2B–E and Figure S3. The average hydrodynamic diameter of Oxa-OA and Oxa-SS-OA NPs was around 90 nm and 100 nm. And the Zeta potential of both Pt(IV) nanoassemblies was -20 mV. (Table S1). The representative TEM images showed that both Pt(IV) NPs displayed uniform spherical morphology with a particle size which is comparable to that established by DLS measurement. Both Oxa-OA and Oxa-SS-OA could self-assemble into NPs in absence of surfactant. Without the aid of DSPE-PEG₂₀₀₀ in the assembly process, increasing size and PDI were observed as shown in Table S1. Given possible undesired stability [27] and *in vivo* drug behavior [30] of non-PEGylated formulations, PEGylated Pt(IV) NPs (described as Oxa-OA NPs and Oxa-SS-OA NPs) were applied for subsequent experiments.

3.3. Colloidal stability

The linkages impose great impact on the assembly manners of prodrug and colloidal stability of nanoparticles. Disulfide bonds between cysteine residues make an essential contribution to the structural stability of proteins [31]. The space flexibility and self-assembly capacity could be greatly improved by the existence of the bond angle or dihedral angle of disulfide bonds which contribute to the stability of proteins or nanoassemblies [21,32]. As shown in Figure S4, the PEGylated prodrug NPs showed impressive colloidal stability with negligible size changes in 10 mM PBS containing 10 % FBS for 12 h. Besides, both Oxa-OA and Oxa-SS-OA NPs remained stable in 5% glucose and RPMI 1640 medium after being stored for seven days at room temperature. (Figure S5)

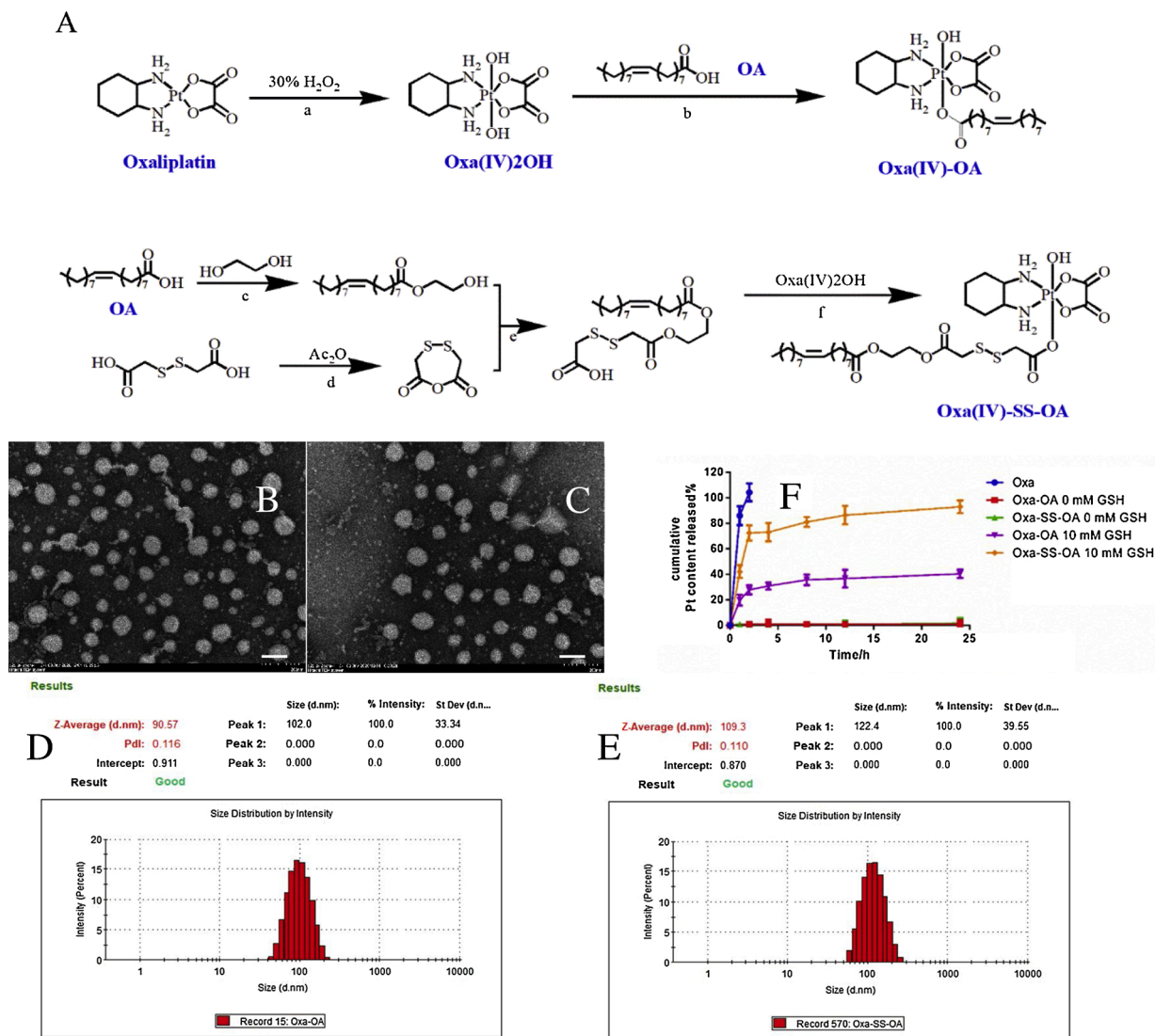


Fig. 2. Synthesis of Pt(IV) prodrugs and characterization of Pt(IV) NPs. (A) Synthesis routes of Oxa-OA and Oxa-SS-OA: (a) 50 °C, 3 h, H₂O₂; (b) EDCI, DMAP, 30 °C, 12 h, DMF; (c) pTsOH, 110 °C, 2 h, reflux; (d) 25 °C, 2 h; (e) EDCI, DMAP, 25 °C, 12 h, CH₂Cl₂; (f) EDCI, DMAP, 30 °C, 12 h, DMF. TEM images of Oxa-OA NPs (B) and Oxa-SS-OA NPs (C) via nano-precipitation method. Scale bar: 100 nm. The nanoparticle size distribution of Oxa-OA NPs (D) and Oxa-SS-OA NPs (E) measured by DLS. (F) Cumulative platinum release profiles of Pt(IV) prodrug nanoparticles in 10 mM PBS 7.4 containing 10 mM GSH determined by ICP-MS.

3.4. *In vitro* drug release

There is a more reducing environment in tumor compared with other normal tissues due to accelerated metabolism and high proliferation rate [33]. The pivotal design of Oxa-SS-OA NPs is their responsiveness to elevated intracellular reductive milieu-interne. To test sensitiveness to GSH, we incubated Pt(IV) NPs in phosphate buffer containing 10 mM GSH for 24 h. As shown in Figs. 2F, little content (less than 2 %) of platinum was detected from Pt(IV) NPs in GSH-free PBS within 24 h indicating appreciable stabilization of prepared NPs, which is consistent with the aforementioned stability study. More than 70 % Pt content that rapidly released from Oxa-SS-OA NPs within 2 h was validated while only 30 % platinum of Oxa-OA NPs was confirmed by ICP-MS. It is indicated that GSH acts as a more efficient cleavage agent to attack disulfide bond but a less powerful reductant to yield active Pt(II). Afterwards, the release of platinum from NPs was moderate as evidence of 40 % and 90 % of drugs released from Oxa-OA NPs and Oxa-SS-OA NPs in 24 h, respectively. Meanwhile, oxaliplatin solution reaches diffusion balance within 2 h. These results indicate that disulfide-bridged Oxa-SS-OA NPs possess superior GSH-response capability over Oxa-OA NPs. It was presumed that reduction of disulfide bond happened prior

to the conversion from Pt(IV) into Pt(II) molecules (oxaliplatin), that is, Oxa-SS-OA NPs revealed cascade reduction-responsive profile of drug release.

3.5. *In vitro* cytotoxicity assay

To investigate cytotoxicity of reduction-responsive Pt(IV) NPs, MTT assays were performed with L-02, RM-1 and 4T1 cells under incubation with Oxa-OA and Oxa-SS-OA NPs. We determined the half-maximal inhibitory concentrations (IC₅₀) according to the MTT assays (Table 1 and Figure S6). Both Pt(IV) prodrugs and NPs showed dose-dependent toxicity in three cell lines. Free oxaliplatin exhibited the most effective cytotoxicity against all cell lines. Pt(IV) prodrugs were less effective in suppressing tumor cell proliferation conceivably due to the delayed release of active oxaliplatin molecule. In cancer cells, RM-1 and 4T1, Oxa-SS-OA showed lower IC₅₀ than Oxa-OA in the form of either free Pt(IV) prodrug or nanoparticle due to more rapid GSH-triggered release of oxaliplatin. While in normal L-02 cells, there was no significant IC₅₀ difference between Pt(IV) groups indicating comparable toxicity in L-02 cell line, which was probably due to the relatively low GSH level. And Oxa-OA also exhibited some cytotoxic activity with extended incubation

Table 1

IC50 value of different Pt formulation in L-02, RM-1 and 4T1 cells.

IC50 (μM)	L-02			RM-1			4T1		
	24h	48h	72 h	24h	48h	72 h	24h	48h	72 h
Oxa sol	60.45	2.321	0.7334	4.709	0.2188	0.1887	10.68	1.253	0.8132
Oxa-OA sol	469.5	264.2	16.55	335.6	26.93	21.99	246.1	35.15	24.27
Oxa-SS-OA sol	144.1	45.77	38.39	132.6	5.050	2.996	77.03	34.51	7.976
Oxa-OA NPs	383.9	86.88	18.58	94.44	11.24	12.81	222.3	35.08	9.594
Oxa-SS-OA NPs	97.33	31.50	11.48	41.54	3.609	2.241	120.3	21.96	2.613

time (72 h) suggesting relatively delayed GSH-responsive hydrolysis of ester bond linked Pt(IV)-fatty acid prodrug as reported [11,34]. Our hypothesis was confirmed by these results that cytotoxicity of Pt(IV) compound highly relies on the release rate of Pt(II) molecules.

3.6. Cell uptake and intracellular Pt accumulation

Motivated by the distinguished cytotoxicity towards cancer cells and normal cells, we further compared cell uptake behavior of Pt(IV) NPs and intracellular drug content in 4T1 cells. As shown in Fig. 3A and B,

Prodrug NPs treated groups exhibited higher intracellular fluorescence intensity observed via CLSM than free C-6 treated at 0.5 and 4 h. The significantly higher cellular uptake efficiency of NPs over free molecules was confirmed. Notably, Oxa-SS-OA NPs presented much stronger intracellular fluorescence intensity than Oxa-OA NPs despite similar nanostructure. Indeed, the phenomenon might be attributed to aggregation-caused quenching (ACQ) effect [35] resulting from encapsulation of fluorescent C-6 into NPs. Oxa-SS-OA NPs are more sensitive to high GSH level and, as a result, more rapidly disassembled in 4T1 cells and more released free C-6 recovered fluorescence than that of Oxa-OA

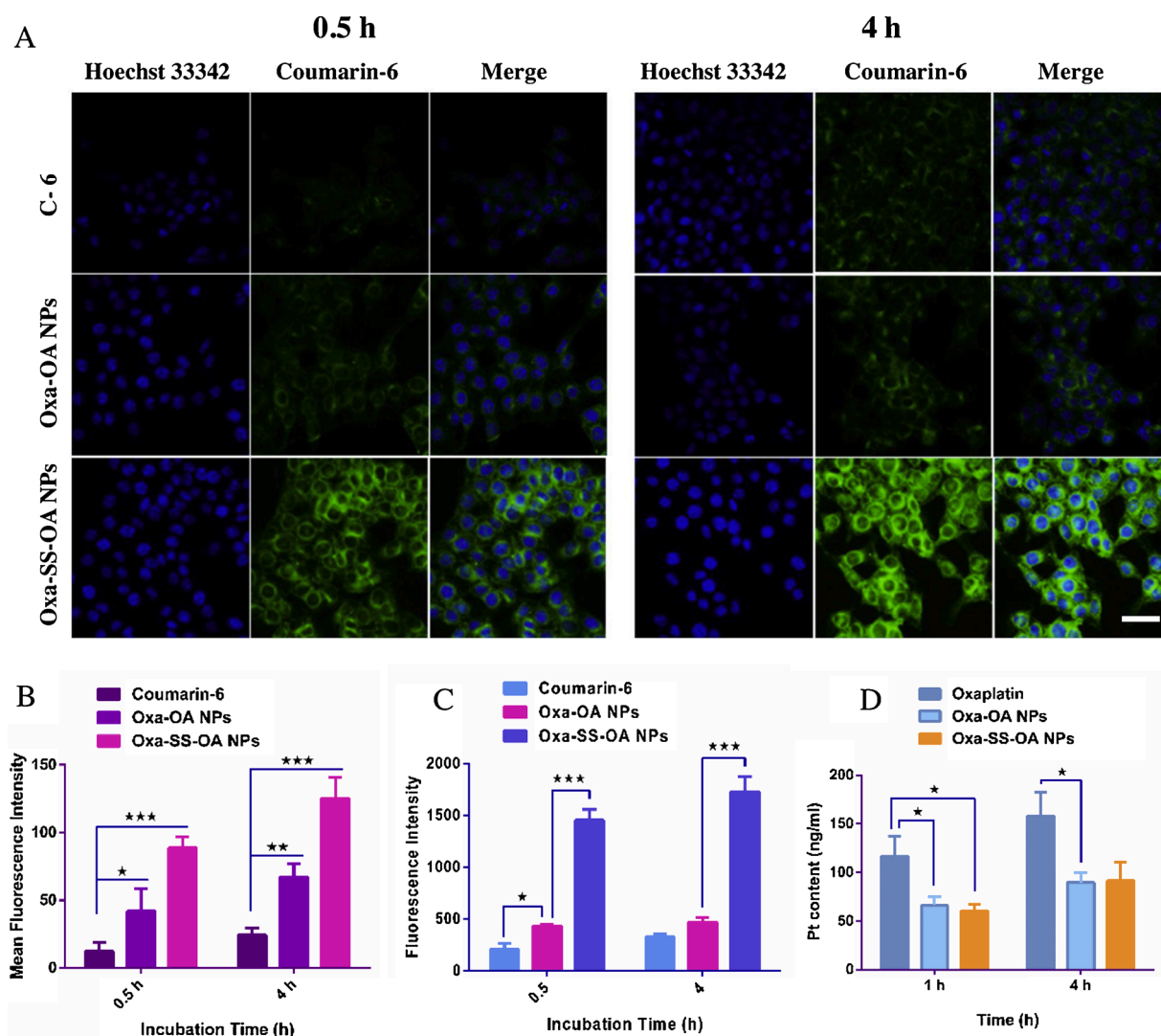


Fig. 3. Cell uptake and intracellular drug accumulation of Pt(IV) NPs in 4T1 cells. (A) Representative images of coumarin-6 encapsulated Pt(IV) NPs in 4T1 cells presented by CLSM. Cells were treated with C-6-labeled Oxa-OA NPs, Oxa-SS-OA NPs and free coumarin-6 for 0.5 or 4 h respectively. scale bar: 20 μm . (B) Quantitative mean fluorescence intensity of CLSM images from different groups. (C) Cellular uptake of the different formulations in 4T1 cells at 0.5 h and 4 h via flow cytometry (n = 3). (D) Intracellular Pt content in 4T1 cells treated by oxaliplatin solution and Pt(IV) NPs was determined by ICP-MS. (* $p < 0.05$, ** $p < 0.01$, *** $p < 0.001$, n = 3).

NPs. The hypothesis was also supported by intracellular platinum content level measured by ICP-MS (Fig. 3D), which showed no significant difference between Oxa-OA and Oxa-SS-OA NPs treated. And free oxaliplatin group revealed most cell uptake probably due to overexpression of associated transporters and relatively efficient internalization. [36–38]

3.7. Determination of GSH and GSSG content inside cells

In the presence of abundant GSH (and other reductants, metallothionein, ascorbate and so on) in cellular milieu, Pt(IV) prodrugs ingested into cells are recovered to Pt(II) compound. [39] The competitive interaction between platinum and GSH plays an important role not only in cellular detoxification but also in drug resistance of Pt-based therapeutics. [40,41] High GSH level can also further affect intracellular processes such as the formation of mRNA, [42] thereby exacerbating oxaliplatin resistance to certain types of cancer. [43] According to most recent reports [34,44], GSH consuming strategies have been into the application to platinum-based drug design for Pt-resistant treatments. As shown in Figure S8, the level of intracellular glutathione decreased significantly after Oxa-SS-OA NPs treated compared with the control. And there was a downward trend of mean GSH level in Oxa-OA group despite no statistical difference compared with control group. Oxa-SS-OA NPs exhibited certain GSH-consuming capacity which might be due to disulfide bond cleavage in terms of our results.

3.8. Determination of nucleus DNA-Pt adduct

For decades, Pt-based antitumor drugs have been widely probed and utilized in oncological practice profiting from potent efficacy against many types of cancer. Though it has been recently reported that Pt complexes play an important role in interaction with RNA [43] and immunogenic cell death inducer [45], the definite and distinctive mechanism of Pt-derived therapeutic drugs is based on the formation of Pt-DNA adducts, interfering with DNA replication and transcription,

which ultimately result in DNA damage and cell death. Therefore, Pt content of DNA-Pt adducts was confirmed by ICP-MS. As shown in Fig. 4A, the highest platinum amount of free oxaliplatin binding to DNA was observed likely owing to relatively more cell uptake and stronger activity over Pt(IV) prodrug NPs. Oxa-SS-OA NPs exhibited superior DNA binding capability over Oxa-OA group suggesting that more oxaliplatin released by GSH-responsive Oxa-SS-OA NPs might contribute to higher DNA-Pt adduct content, probably leading to more effective cytotoxicity.

3.9. In vivo pharmacokinetics

To evaluate the pharmacokinetic profiles of Pt(IV) NPs, SD rats were adopted and i.v. administrated via tail vein injection. The Pt content-time curves were illustrated in Fig. 4B and the pharmacokinetic parameters were showed in Table 2. With around threefold higher AUC values than free oxaliplatin, both Pt(IV) prodrug NPs significantly extended the circulation time against blood clearance in comparison to oxaliplatin solution indicating rapid clearance of free drug. Slower clearance rate of Pt(IV) NPs as compared to oxaliplatin solution indicated favorable stabilization against physicochemical elimination in the bloodstream. The amount of drug release in the blood of Oxa-OA NPs and Oxa-SS-OA NPs is basically equal, indicating that both nano-assemblies are relatively stable in the blood circulation.

3.10. In vivo biodistribution

The biodistribution of Pt(IV) prodrug NPs in 4T1 tumor-bearing mice was also determined by ICP-MS. As illustrated in Fig. 4C and D, Pt(IV) NPs mainly accumulated in liver and spleen after intravenous administration which was due to elimination by reticuloendothelial system (RES). And free oxaliplatin was significantly more distributed in the main organs, especially kidney, than Pt(IV) NPs groups, which might be a cue of nephrotoxicity, the main dose-limiting toxicity of platinum drugs in clinic [6,40]. Notably, Pt level in tumors at 1 and 4 h after

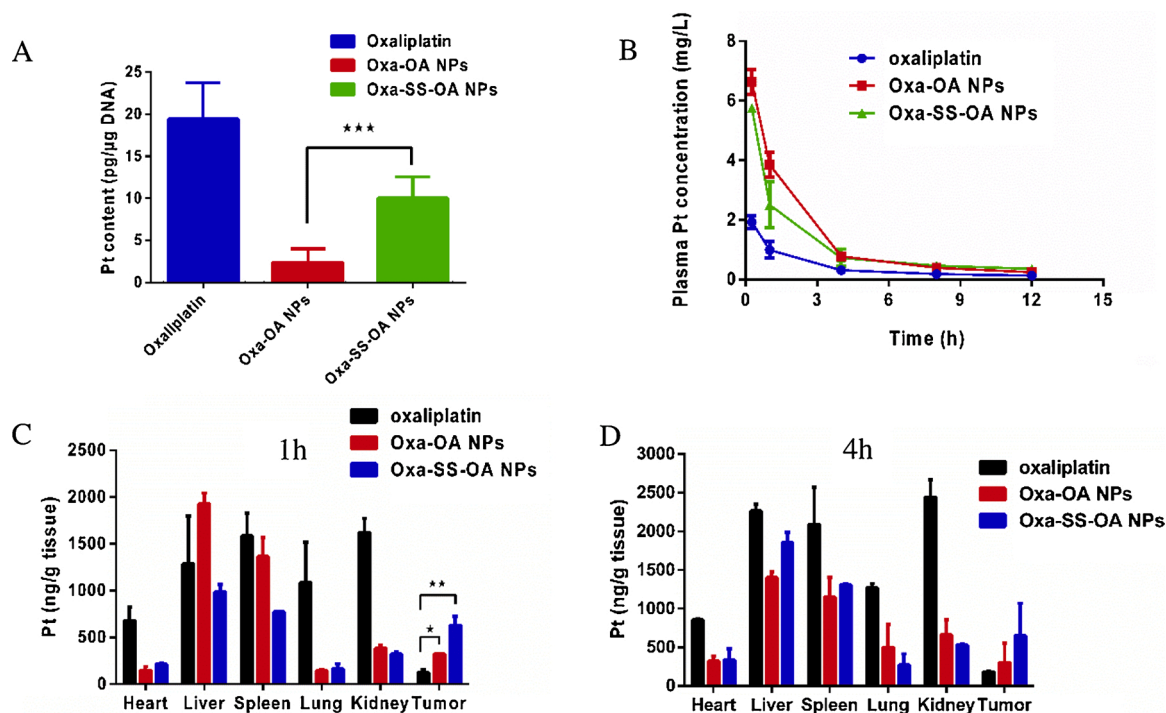


Fig. 4. (A) DNA binding Pt content in 4T1 cells treated with oxaliplatin, Oxa-OA NPs and Oxa-SS-OA NPs for 12 h. (ns: no significant difference; * $p < 0.05$, ** $p < 0.01$, *** $p < 0.001$, $n = 3$). (B) Mean plasma Pt concentration-time profiles of oxaliplatin solution, Oxa-OA NPs and Oxa-SS-OA NPs after i.v. administration in SD rats. Biodistribution of oxaliplatin solution, Oxa-OA NPs and Oxa-SS-OA NPs in 4T1 tumor-bearing Balb/c mice ($n = 3$) at 4 h (C) and 12 h (D).

Table 2
Pharmacokinetic parameters of oxaliplatin solution and Pt(IV) prodrug NPs.

Formulations	AUC _{0-12 h} ^{a)}	t _{1/2} ^{b)}	CL ^{c)}	V ^{d)}
oxaliplatin solution	5.151 ± 0.606	3.686 ± 1.857	0.529 ± 0.019	2.845 ± 1.538
Oxa-OA NPs	16.19 ± 1.554 ^A	3.226 ± 1.517	0.177 ± 0.015 ^A	0.829 ± 0.411
Oxa-SS-OA NPs	13.34 ± 1.969 ^A	9.591 ± 5.652	0.173 ± 0.033 ^A	2.261 ± 1.260

a) Area under the plasma concentration-time curve (mg h L⁻¹).

b) Half-life (h).

c) clearance rate (L h⁻¹ kg⁻¹).

d) Apparent volume of distribution (L kg⁻¹). A: p < 0.001, versus oxaliplatin solution as the control. (Two-tailed Student's t-test). Data are presented as mean ± SD.

injection showed that both Oxa-OA NPs and Oxa-SS-OA NPs, to a larger extent, accumulated in tumor than free oxaliplatin, indicating the enhanced retention of NPs in tumor as reported [46]. These results showed that Pt(IV) prodrug NPs in the blood are more stable and their tumor-specific distributions are higher than oxaliplatin solution, which does not tend to cause obvious toxic reaction or severe side effects.

3.11. *In vivo* antitumor efficacy and systematic toxicity investigation

Then we investigated the efficacy of Pt(IV) NPs using 4T1 xenograft model of Balb/c mice treated by tail intravenous injection of different formulations. As illustrated in Fig. 5A, maximum tolerated dose was determined as 6 mg Pt/kg for oxaliplatin solution and 20 mg Pt/kg for Pt(IV) NPs (Oxa-OA NPs and Oxa-SS-OA NPs). While the mice body weight of 10 mg/kg oxaliplatin group declined dramatically compared with the other groups. Oleic acid-based drug delivery systems possess great potential in elevating Pt-formulation dosage safely in traditional chemotherapy. As presented in Fig. 5B-C and Figure S9, obviously disulfide bond-bridged Oxa-SS-OA NPs revealed more potent efficacy than 5% glucose and oxaliplatin solution with significantly shrinking tumor size. In comparison, non-sensitive Oxa-OA NPs exhibited a more rapid tumor proliferation rate in bulk volume, possibly caused by the less drug release in tumor site. Further, Oxa-SS-OA NPs showed better activity suppressing tumor growth than Oxa-OA NPs at equal dosage (6 mg/kg), probably on account of more sensitive GSH-response, distinctive Pt

release manner and tumor accumulation. As for systematic toxicity investigation, all Pt(IV) NPs group showed no significant difference in body weight fluctuation compared with the control group (Fig. 5D). Histological analysis of various tissues was performed to investigate the pathological feature in main organs harvested from Balb/c mice. According to the results of H&E staining (Fig. 6A), there was no significant changes in the structure of heart, liver, spleen, lung and kidney between all different formulations treated group and 5% glucose group. And to figure out the effect of Pt(IV) NPs on hepatorenal function, indicators of ALT, AST, BUN and CREA were measured. In presence of Fig. 6B, values did not differ significantly in all groups compared to 5% glucose except for oxaliplatin solution with higher AST than control group. To sum up, disulfide-based oleic acid covalently tethered Pt(IV) prodrug delivery system presented unique advantages on antitumor activity and *in vivo* safety benefiting from selective intracellular rapid drug release via GSH-triggered disulfide cleavage, which retains impressive application potential for future.

3.12. Behavioral assessment of mechanical hypersensitivity

Oxaliplatin-based chemotherapy can achieve high rates of survival in patients with specific types of cancer but usually causes severe neuropathy, which limits the maximum safe dose of oxaliplatin and its clinical outcome [6,47]. Sensory disorders induced by oxaliplatin, including pain and paraesthesia, greatly compromise the quality of

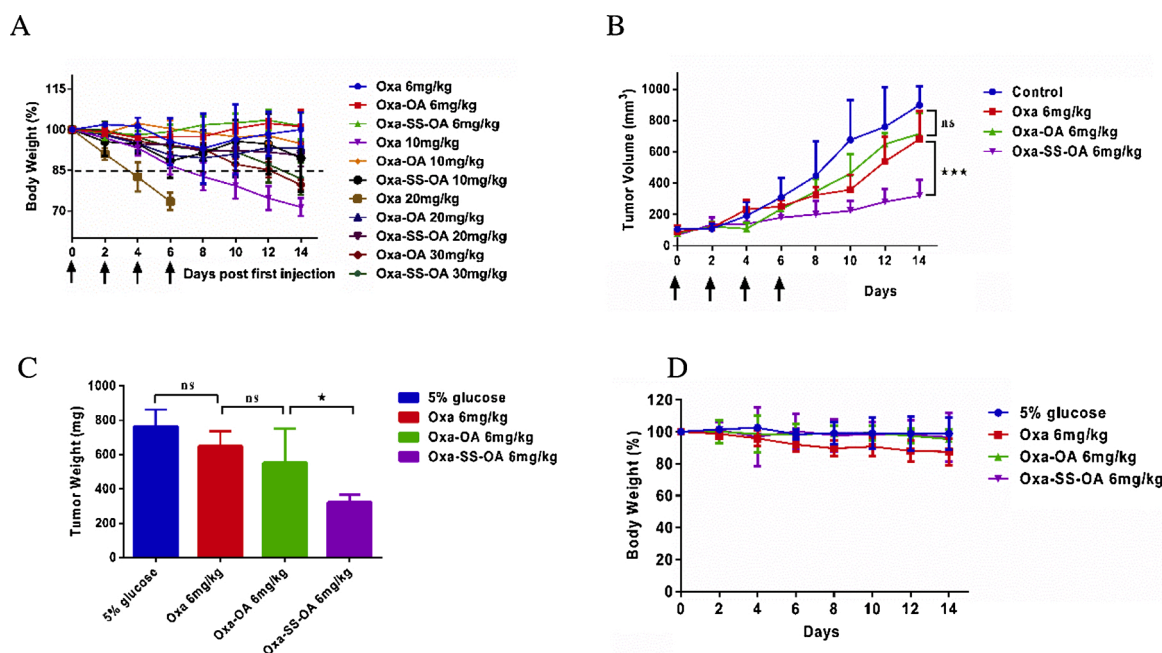


Fig. 5. The antitumor efficacy *in vivo*. (A) Maximum tolerated dose (MTD) of oxaliplatin solution, Oxa-OA NPs and Oxa-SS-OA NPs determined by continuous *i.v.* injection of a series of doses. The arrow indicates the day of dosing different formulation *via* tail vein injection. Body weights of mice were monitored and the maximal dosage administrated by mice group was determined as MTD if mice remain more than 85 % mean weights compared with the first day. The tumor volume (B), tumor weight (C) and body weight (D) of 4T1 tumor-bearing Balb/c mice (n = 6). The arrow indicates the day of dosing different formulation *via* tail vein injection. (ns: significant difference; *p < 0.05, **p < 0.01, ***p < 0.001, n = 3).

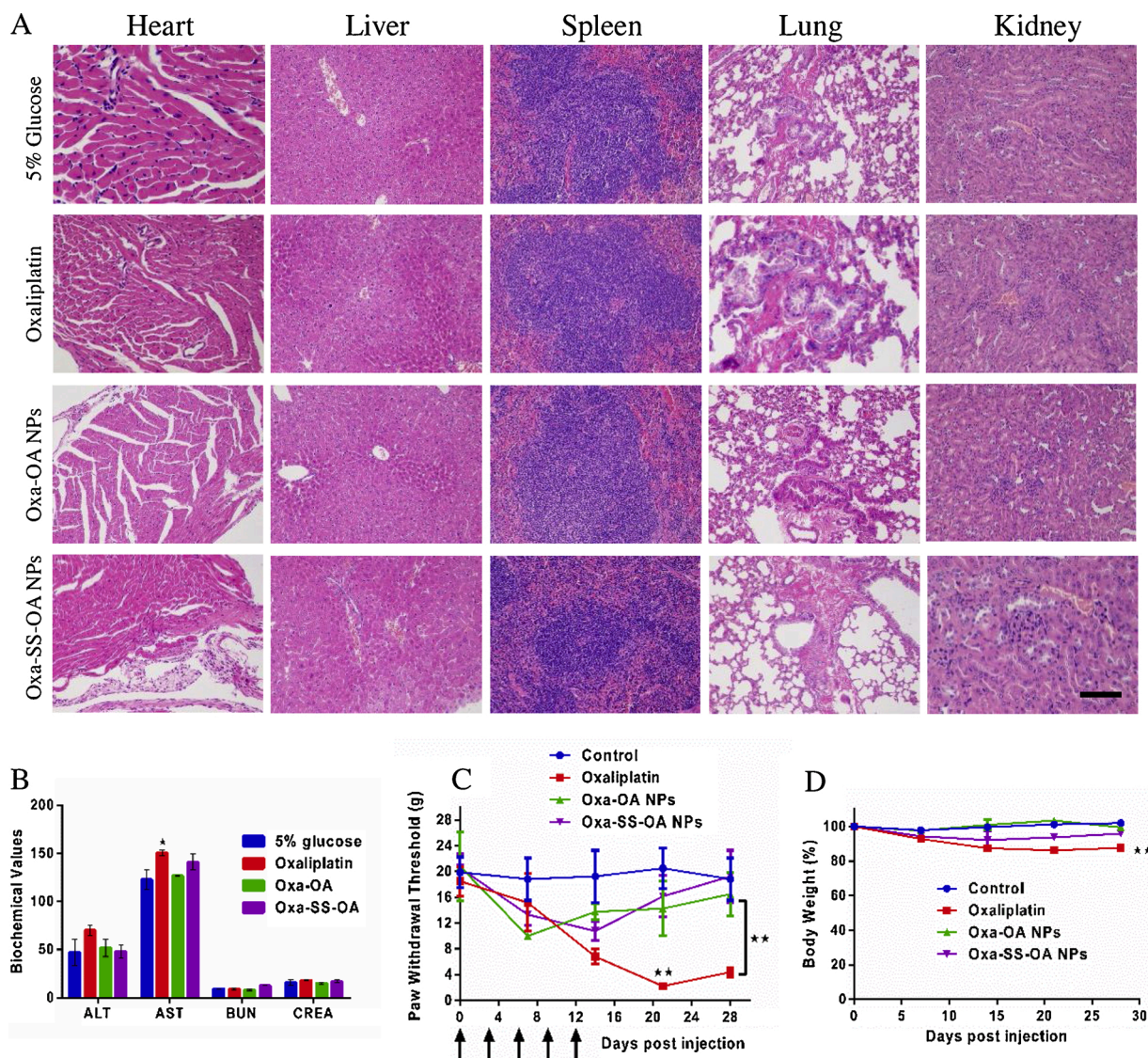


Fig. 6. (A) Histopathological section (H&E staining) of the hearts, livers, spleens, lungs and tumors of Balb/c mice after different formulations administration. scale bar: 100 μ m. (B) Liver (ALT, AST) and kidney (CR, BUN) functional parameters at day 14 after mice were sacrificed. (C) Threshold (g) of withdrawal response during mechanical stimuli of oxaliplatin and Pt(IV) NPs treated rats. (D) Body weight change in each group after the first injection. (* $p < 0.05$, ** $p < 0.01$, versus oxaliplatin group as the control).

patients' life for months or even years [48]. To evaluate the effect of Pt(IV)-oleic acid prodrug NPs on peripheral neurotoxicity, mechanical paw withdrawal threshold (PWT) was measured on SD rats. PWT was lower in oxaliplatin administrated rats than that in 5% glucose group at about two weeks since first injection (Fig. 6C). In addition, Oxa-OA NPs and Oxa-SS-OA NPs treated rats lost weight moderately after injection and returned to a similar level of control group within four weeks, with a significant difference of body weight occurred between Pt(IV) NPs and oxaliplatin solution at day 28 (Fig. 6D). It's worth noting that oxaliplatin solution treated rats lost more weight than that Pt(IV) NPs treated and control group at last measurement. The results of mechanical hypersensitivity assessment demonstrate that Pt(IV)-OA NPs can alleviate the peripheral neurotoxicity and systematic toxicity caused by oxaliplatin.

4. Conclusion

In summary, we have developed a platinum-based nanoassembly drug delivery platform, which is relied on elevated intracellular GSH level in tumor site and sensitive cleavage of disulfide bond in Pt(IV) prodrug. *In vitro* and *in vivo* assays demonstrated that oleic acid tethered

Pt(IV) prodrug NPs had higher antitumor activity and lower side effects than oxaliplatin. Furthermore, disulfide-guided Oxa-SS-OA NPs exhibited higher anticancer potency compared with ester bond linked Oxa-OA NPs. Disulfide bond endows oxaliplatin-oleic acid prodrug with rapid cascade release of oxaliplatin and lower IC₅₀ in cancer cells, and self-assembly delivery system enables high drug efficiency, prolonged blood circulation and high tumor accumulation of platinum. The attempt to introduce disulfide bond into Pt(IV)-fatty acids prodrug is of great significance to reasonable application of platinum-based drugs. Disulfide bond-guided cascade reduction-responsive self-assembly system presents a broad prospect in clinical application.

CRediT authorship contribution statement

Xiao Kuang and Yongjun Wang: conceived the project. Xiao Kuang, Chunlin Guo and Dongxu Chi: synthesized and characterized the prodrugs. Xiao Kuang, Jinbo Li, Yinxian Yang, Shuang Zhou, Cong Luo, Hongzhuo Liu, Zhonggui He and Dongxu Chi: carried out the experiments. Xiao Kuang and Dongxu Chi: analyzed the data and wrote the manuscript. Xiao Kuang and Yongjun Wang: participated in

the manuscript revision. All authors discussed the results and reviewed the manuscript.

Declaration of Competing Interest

The authors declare that they have no known competing financial interests or personal relationships that could have appeared to influence the work reported in this paper.

Acknowledgement

This research was supported by the Career Development Program for Young and Middle-aged Teachers in Shenyang Pharmaceutical University (Shenyang, China).

Appendix A. Supplementary data

Supplementary material related to this article can be found, in the online version, at doi:<https://doi.org/10.1016/j.colsurfb.2021.111766>.

References

- Galanski, M.A. Jakupec, B.K. Keppler, Update of the preclinical situation of anticancer platinum complexes: novel design strategies and innovative analytical approaches, *Curr. Med. Chem.* 12 (2005) 2075–2094.
- Y.R. Zheng, K. Suntharalingam, T.C. Johnstone, et al., Pt(IV) prodrugs designed to bind non-covalently to human serum albumin for drug delivery, *J. Am. Chem. Soc.* 136 (24) (2014) 8790–8798.
- S. Mitragotri, P.A. Burke, R. Langer, Overcoming the challenges in administering biopharmaceuticals: formulation and delivery strategies, *Nat. Rev. Drug Discov.* 13 (9) (2014) 655–672.
- H.S. Oberoi, N.V. Nukolova, A.V. Kabanov, et al., Nanocarriers for delivery of platinum anticancer drugs, *Adv. Drug Deliv. Rev.* 65 (13–14) (2013) 1667–1685.
- J.L.H. Hartmann, Toxicity of platinum compounds, *Expert Opin. Pharmacother.* 4 (6) (2003) 889–901.
- A. Avan, T.J. Postma, C. Ceresa, et al., Platinum-induced neurotoxicity and preventive strategies: past, present, and future, *Oncologist* 20 (4) (2015) 411–432.
- N.J. Wheate, S. Walker, G.E. Craig, et al., The status of platinum anticancer drugs in the clinic and in clinical trials, *Dalton Trans.* 39 (35) (2010) 8113–8127.
- H.Han Catherine, P.K. Dean, H. Kilfoyle, Andrew Hill, Mark J. Mckeage, Phase I drug-interaction study of effects of calcium and magnesium infusions on oxaliplatin pharmacokinetics and acute neurotoxicity in colorectal cancer patients, *BMC Cancer* 13 (2013) 495.
- H. Huang, Y. Dong, Y. Zhang, et al., GSH-sensitive Pt(IV) prodrug-loaded phase-transitional nanoparticles with a hybrid lipid-polymer shell for precise theranostics against ovarian cancer, *Theranostics* 9 (4) (2019) 1047–1065.
- C. Huang, Y. Sun, M. Shen, et al., Altered cell cycle arrest by multifunctional drug-loaded enzymatically-triggered nanoparticles, *ACS Appl. Mater. Interfaces* 8 (2) (2016) 1360–1370.
- T. Fang, Z. Ye, J. Wu, et al., Reprogramming axial ligands facilitates the self-assembly of a platinum(IV) prodrug: overcoming drug resistance and safer in vivo delivery of cisplatin, *Chem. Commun. (Camb.)* 54 (66) (2018) 9167–9170.
- T.C. Johnstone, K. Suntharalingam, S.J. Lippard, The next generation of platinum drugs: targeted Pt(II) agents, nanoparticle delivery, and Pt(IV) prodrugs, *Chem. Rev.* 116 (5) (2016) 3436–3486.
- S. He, C. Li, Q. Zhang, et al., Tailoring platinum(IV) amphiphiles for self-targeting all-in-One assemblies as precise multimodal theranostic nanomedicine, *ACS Nano* 12 (7) (2018) 7272–7281.
- F. Chen, X. Huang, M. Wu, et al., A CK2-targeted Pt(IV) prodrug to disrupt DNA damage response, *Cancer Lett.* 385 (2017) 168–178.
- H. Kostrhunova, J. Zajac, L. Markova, et al., A multi-action Pt(IV) conjugate with oleate and cinnamate ligands targets human epithelial growth factor receptor HER2 in aggressive breast Cancer cells, *Angew. Chem. Int. Ed. Engl.* (2020).
- T.V.O.H. Sang-Min Lee, Sonbinh T. Nguyen, Polymer-caged nanobots for synergistic cisplatin-doxorubicin combination chemotherapy, *J. Am. Chem. Soc.* 132 (2010) 17130–17138.
- F.Q. Schafer, G.R. Buettner, Redox environment of the cell as viewed through the redox state of the glutathione disulfide/glutathione couple, *Free Radic. Biol. Med.* 30 (11) (2001) 1191–1212.
- M.H. Lee, Z. Yang, C.W. Lim, et al., Disulfide-cleavage-triggered chemosensors and their biological applications, *Chem. Rev.* 113 (7) (2013) 5071–5109.
- M.G. Lorine Brülisauer, Jean-Christophe Leroux, Disulfide-containing parenteral delivery systems and their redox-biological fate, *J. Control. Release* (2014).
- Y. Yang, B. Sun, S. Zuo, et al., Trisulfide bond-mediated doxorubicin dimeric prodrug nanoassemblies with high drug loading, high self-assembly stability, and high tumor selectivity, *Sci. Adv.* 6 (45) (2020).
- Y. Wang, D. Liu, Q. Zheng, et al., Disulfide bond bridge insertion turns hydrophobic anticancer prodrugs into self-assembled nanomedicines, *Nano Lett.* 14 (10) (2014) 5577–5583.
- B. Sun, C. Luo, H. Yu, et al., Disulfide bond-driven oxidation- and reduction-responsive prodrug nanoassemblies for Cancer therapy, *Nano Lett.* 18 (6) (2018) 3643–3650.
- C. Luo, J. Sun, D. Liu, et al., Self-assembled redox dual-responsive prodrug-nanosystem formed by single thioether-bridged paclitaxel-fatty acid conjugate for Cancer chemotherapy, *Nano Lett.* 16 (9) (2016) 5401–5408.
- B. Sun, C. Luo, X. Zhang, et al., Probing the impact of sulfur/selenium/carbon linkages on prodrug nanoassemblies for cancer therapy, *Nat. Commun.* 10 (1) (2019) 3211.
- R.T. Holman, Measurement of polyunsaturated fatty acids, *Methods Biochem. Anal.* 4 (1957) 99–138.
- B. Sun, C. Luo, W. Cui, et al., Chemotherapy agent-unsaturated fatty acid prodrugs and prodrug-nanoplatforams for cancer chemotherapy, *J. Control. Release* 264 (2017) 145–159.
- C. Luo, J. Sun, B. Sun, et al., Facile fabrication of tumor redox-sensitive nanoassemblies of small-molecule oleate prodrug as potent chemotherapeutic nanomedicine, *Small* 12 (46) (2016) 6353–6362.
- F. Miao, R. Wang, G. Cui, et al., Engagement of MicroRNA-155 in exaggerated oxidative stress signal and TRPA1 in the dorsal horn of the spinal cord and neuropathic pain during chemotherapeutic oxaliplatin, *Neurotox. Res.* 36 (4) (2019) 712–723.
- P. Bougnoux, N. Hajjaji, K. Maheo, et al., Fatty acids and breast cancer: sensitization to treatments and prevention of metastatic re-growth, *Prog. Lipid Res.* 49 (1) (2010) 76–86.
- J. Wang, W.M. L.L. Lock, J. Tang, M. Sui, W. Sun, H. Cui, D. Xu, Y. Shen, The role of Micelle Size in tumor accumulation, penetration, and treatment, *ACS Nano* 28 (7) (2015).
- N.L. Haworth, J.E. Gready, R.A. George, et al., Evaluating the stability of disulfide bridges in proteins: a torsional potential energy surface for diethyl disulfide, *Mol. Simul.* 33 (6–8) (2007) 475–485.
- Yinxian Yang, B.S. Shiyi Zuo, Ximu Li, Shuang Zhou, Lingxiao Li, Cong Luo, Hongzhuo Liu, Maosheng Cheng, Yongjun Wang, Shujun Wang, Zhonggui He, Jin Sun, Trisulfide bond-mediated doxorubicin dimeric prodrug nanoassemblies with high drug loading, high self-assembly stability, and high tumor selectivity, *Science Advance* (2020).
- J.M. Brown, Tumor microenvironment and the response to anticancer therapy, *Cancer Biol. Ther.* 1 (5) (2002) 453–458.
- X. Ling, J. Tu, J. Wang, et al., Glutathione-responsive prodrug nanoparticles for effective drug delivery and Cancer therapy, *ACS Nano* 13 (1) (2019) 357–370.
- J. Qi, X. Hu, X. Dong, et al., Towards more accurate bioimaging of drug nanocarriers: turning aggregation-caused quenching into a useful tool, *Adv. Drug Deliv. Rev.* 143 (2019) 206–225.
- S. Schoch, S. Gajewski, J. Rothfuss, et al., Comparative study of the mode of action of clinically approved platinum-based chemotherapeutics, *Int. J. Mol. Sci.* 21 (18) (2020).
- A.K. Holzer, G.H. Manorek, S.B. Howell, Contribution of the major copper influx transporter CTR1 to the cellular accumulation of cisplatin, carboplatin, and oxaliplatin, *Mol. Pharmacol.* 70 (4) (2006) 1390–1394.
- C. Indiveri, M. Galluccio, M. Scalise, et al., Strategies of bacterial over expression of membrane transporters relevant in human health: the successful case of the three members of OCTN subfamily, *Mol. Biotechnol.* 54 (2) (2013) 724–736.
- E. Wexselblatt, D. Gibson, What do we know about the reduction of Pt(IV) prodrugs? *J. Inorg. Biochem.* 117 (2012) 220–229.
- L. Kelland, The resurgence of platinum-based cancer chemotherapy, *Nat. Rev. Cancer* 7 (8) (2007) 573–584.
- N. Vasan, J. Baselga, D.M. Hyman, A view on drug resistance in cancer, *Nature* 575 (7782) (2019) 299–309.
- Y. Wang, J. Tang, Y. Yang, et al., Functional nanoparticles with a reducible tetrasulfide motif to upregulate mRNA translation and enhance transfection in hard-to-Transfect cells, *Angew. Chem. Int. Ed. Engl.* 59 (7) (2020) 2695–2699.
- P.M. Bruno, Y. Liu, G.Y. Park, et al., A subset of platinum-containing chemotherapeutic agents kills cells by inducing ribosome biogenesis stress, *Nat. Med.* 23 (4) (2017) 461–471.
- Y. Xu, X. Han, Y. Li, et al., Sulforaphane mediates glutathione depletion via polymeric nanoparticles to restore cisplatin chemosensitivity, *ACS Nano* 13 (11) (2019) 13445–13455.
- M.J.R. Tham, M.V. Babak, W.H. Ang, Platin ER: a Highly Potent Anticancer Platinum(II) Complex that induces Endoplasmic Reticulum Stress-driven Immunogenic Cell Death, *Angew. Chem. Int. Ed. Engl.* (2020).
- S. Sindhvani, A.M. Syed, J. Ngai, et al., The entry of nanoparticles into solid tumours, *Nat. Mater.* 19 (5) (2020) 566–575.
- S.N. Housley, P. Nardelli, D.I. Carrasco, et al., Cancer exacerbates chemotherapy-induced sensory neuropathy, *Cancer Res.* 80 (13) (2020) 2940–2955.
- K.M. Huang, A.F. Leblanc, M.E. Uddin, et al., Neuronal uptake transporters contribute to oxaliplatin neurotoxicity in mice, *J. Clin. Invest.* 130 (9) (2020) 4601–4606.